CZECH TECHNICAL UNIVERSITY IN PRAGUE

DOCTORAL THESIS STATEMENT

CZECH TECHNICAL UNIVERSITY IN PRAGUE
Faculty of Civil Engineering
Department of Mechanics

Ing. Jan Stránský

MESOSCALE DISCRETE ELEMENT MODEL FOR CONCRETE AND ITS COMBINATION WITH FEM

Ph.D Programme: **Civil Engineering**
Branch of study: **Physical and Material Engineering**

Doctoral thesis statement for obtaining the degree of „Doctor“, abbreviated to „Ph.D.”

Prague, January, 2018

Contents

1 Introduction

Concrete is a composite material composed of inclusions (gravel and sand aggregates) embedded in a cement (or similar binder) matrix and is the most widely used building material. Therefore it has been in various contexts subjected to extensive research. In practical civil engineering, concrete is usually idealized as a homogeneous isotropic material. However, certain applications require description of concrete on lower than structural scales and heterogeneity (e.g, presence of aggregates) has to be taken into account.

The basic behavior and structural response of concrete structures may be described analytically (for example a beam structure in the elastic range). Introducing more and more enhancements and features of the models leads to analytical unsolvability and numerical methods, usually with the help of computers, have to be introduced.

Numerical simulations are an indispensable part of the current engineering and science development. For different engineering areas there are different numerical methods used. In solid phase mechanics, the leading methods are the finite element method (FEM) and the discrete (distinct) element method (DEM).

Usually, the solution is performed by a computer program, which is focused on a narrower or wider class of problems (such as solid mechanics, fluid dynamics, heat analysis, DEM etc.). If a combination of two classes of problems is required (coupling of mechanical and heat analysis for instance), it is often possible to find a code allowing such approach. However, in some cases, there exists no program that can solve the desired combination of problems. One possible approach to deal with such situation would be to write a new or extend an existing program implementing the requested features. Another possible approach would be to use existing independently developed codes, each one focused on a specific class of problems, and “glue” them together.

There are countless software programs for both FEM and DEM. In this thesis, coupling of FEM code OOFEM and DEM code YADE is described and illustrated.

1.1 Objectives of the thesis

1. To investigate basic properties of particle models, namely the relation between micro- and macroscopic elastic properties of random dense packings in terms of analytical formulas and results of numerical simulations. Preparation and properties of random dense packings should be investigated beforehand.

2. To develop open source tools for combination of the discrete element method and the finite element method. Several classes of combination approaches together with simple examples should be addressed.

3. To develop a mesoscale discrete element model for concrete. The model should take into account the effect of aggregates and the interfacial transition zone (ITZ) between aggregates and the matrix. The model should be validated against experimental data from available literature.

2 State of the art

2.1 Discrete stress

The evaluation of equivalent stress from discrete forces is a topic much older than DEM itself [31] described in many papers [1, 13, 4], but until these days it is a subject of debates in specialized literature [7, 3, 29, 5, 6]. A brief summary of current knowledge and author's new ideas are presented in this chapter.

The discrete elements in DEM possess 6 degrees of freedom, namely 3 displacements and 3 rotations. Classical Boltzmann continuum assumes 3 degrees of freedom (3 displacements) in each material point. Therefore a higher order (Cosserat for instance) model should be used for continuum approximation of DEM in its general form [1].

2.2 DEM–FEM coupling

2.2.1 Surface coupling

The so called surface coupling [34, 18, 32] is probably the most straightforward FEM–DEM coupling strategy.

The principle is to split the whole problem into two separated domains, one modeled by FEM and the other by DEM. As an illustrative example, consider a steel beam modeled by FEM falling into an assembly of gravel particles modeled by DEM. Both domains interact with each other, but are physically separated during the entire time of the process.

2.2.2 Volume coupling

Volume coupling [37, 46, 2, 44] is similar to the surface coupling. The difference is that the two subdomains overlap each other.

The possible usage of this approach could be a model of concrete beam subjected to an impact load (blast for example). The whole beam would be modeled by FEM and only a small volume of the concrete (the volume to be fragmented and crushed) would be modeled by DEM. To preserve continuous nature of the beam, a transition zone (containing both FEM and DEM) would be included.

There are two basic strategies how to model transition between FEM and DEM domains [46]. The first one, "direct" or "master/slave" method [2], considers DEM particles overlapping with FEM as direct slaves of the FEM mesh (using standard "master/slave" or "hanging nodes" approach). The second one, the "weak" or "Arlequin" method [37, 44], considers a transition bridging zone, where the total response is superposed from contributions of the two models and is interpolated between both domains. In the thesis, only the former (master/slave) approach is described.

2.2.3 Multiscale coupling

The idea of multiscale simulations is to model the problem on the large (macro) scale using information from a lower (micro) scale [36, 44]. In the current context, the (first order) homogenization [21] is presented.

Geometric information (strain) from macro scale – integration points (IPs) of FEM mesh – is transferred to the micro scale (representative volume element - RVE - modeled by DEM). On the micro scale, the boundary value problem (BVP) governed by the transferred prescribed strain is solved using periodic boundary conditions [40]. The output of the micro-scale problem is the stress tensor (sufficient for explicit solution scheme) and possibly also the constitutive characteristics (stiffness tensor, needed by implicit solution schemes), which are transferred back to the macro-scale problem.

2.2.4 Contact coupling

The idea of contact analysis [19] is very simple and opposite to the multiscale approach. The material on the large scale is considered to be of a particulate nature and is modeled by particles using DEM. Each such particle is deformable and further modeled by FEM.

There is no strict border between the cases when the solution can be considered as a contact FEM analysis and when it is already DEM. For only a few particles we would probably use the former one, but when the number of particles increases, the DEM modeling (with its efficient contact detection algorithms) would be more appropriate. This strategy can be actually considered as full FEM, only the contact detection is “borrowed” from the DEM program.

2.2.5 Sequential coupling

The classification complementary to the concurrent combination is the sequential approach. It assumes that the processes are separable in time and therefore only the former process influences the latter process but not vice versa Usually some kind of homogenization techique is used to determine FEM model parameters at the beginning of the latter process from the final state of former process.

2.3 Discrete mesoscale model for concrete

Various approaches of mesoscale concrete modeling have been published. All of them consider concrete as a matrix-based composite with aggregates as inclusions, possibly also with pores. The approaches may be classified from several points of view.

The first significant difference is whether the model is formulated in two dimensions (see, e.g., [25, 35, 39, 43, 47, 23]) or in three dimensions (see, e.g., [41, 45, 28, 11, 14, 16, 15]). Although the 3D models describe the heterogeneous geometry more realistically, some ideas and approaches from 2D models may be useful and applicable also for the 3D case.

According to the numerical method used, the approaches can be divided into continuum and discrete based. Although the main purpose of this work is to develop a discrete mesoscale model, continuum based approaches can be very inspiring, especially in the context of ITZ material models.

The discrete element method can model disintegration of materials and is therefore also very popular in the context of concrete modeling, especially for scenarios like fragmentation, impact or explosion problems etc. How DEM is used for mesoscale concrete modeling, see, e.g., [12, 24, 26, 27, 41, 43, 23, 14, 16, 15].

2.3.1 Mesoscale geometry

The concrete heterogeneous geometry plays an important role in the realistic description of concrete mesoscale behavior. The authors use various ways of definition of aggregate geometry, from extremely simplified regular uniformly sized hexagonal particles through commonly used spherical/circular (see, e.g., [35, 43, 45, 47, 28, 23, 16, 15]) or ellipsoidal/elliptical (see, e.g., [24, 25, 28]) representation to more sophisticated approximation by polygons/polyhedrons [30, 35, 28] or representation of aggregates by the series of harmonic functions [20, 25, 38].

For method testing and validation, there also exist experiments with artificially created mesoscale geometries, where large aggregates have predefined size, position and orientation, see [42, 10]. The aggregates are modeled as one rigid particle [43, 16, 15] or as a cluster of particles/elements (e.g., spheres in DEM) [23, 24, 28]. Such clustered particles may be rigid or deformable.

2.3.2 Material models for mortar and aggregates

For practical and computational reasons, both matrix and individual aggregates are modeled as homogeneous components. Some authors (e.g., [11, 14, 23]) consider aggregates as non damageable, so cracks and damage can only propagate in the matrix. This assumption is reasonable for certain loading scenarios, but is not applicable in a general case, where cracks can propagate also through aggregates (e.g., for light-weight concrete or for dynamic loading).

Although all three phases of concrete composite material may be modeled with different material models [47], many authors use for matrix, aggregates and ITZ the same material model [24, 28, 39, 43].

In the case of continuous (FEM) models, the material model for matrix and aggregates is usually based on damage-plasticity models. The discrete models usually work with a more or less complex contact law and a link failure envelope. See, e.g., [27, 41, 43].

2.3.3 Interface transition zone

Apart from separated matrix and aggregates, the interface between these components needs to be properly specified for realistic modeling of inelastic processes (crack initiation and propagation for instance). The interface is a very special region of concrete, occupying a minimal volume, but having a significant influence on resulting concrete properties.

The special role of ITZ is given by both mechanical and chemical reasons, being investigated mathematically and experimentally [17, 22].

From the simulation point of view, the ITZ is often described by the same type of material model as the other constituents, but is considered as the weakest part of the concrete composite, which is reflected in the material parameters choice.

3 Results

3.1 Elastic properties of particle models

The numerical relation between macro- and microscopic parameters has been computed for several values of ι_r and compared to the analytical values

$$\mathbb{D}_e = \frac{1}{V}\sum_c L^c A^c \left(\bar{E}\mathbb{N}^c + \bar{G}\mathbb{T}^c\right) \tag{3.1}$$

and

$$E = \frac{\sum L^c A^c}{3V} \cdot \frac{\bar{E}\left(2\bar{E}+3\bar{G}\right)}{4\bar{E}+\bar{G}} \qquad \nu = \frac{\bar{E}-\bar{G}}{4\bar{E}+\bar{G}}. \tag{3.2}$$

In graphs, points represent numerically obtained data and data according to analytical estimation of full elastic stiffness tensor. The line represents the analytical estimation of Young's modulus and Poisson's ratio.

The numerical results of static FEM, quasi-static DEM simulations and analytical full stiffness tensor are practically indistinguishable from each other. Certain discrepancy can be found for larger values of $\bar{G}/\bar{E} \to \infty$ because then Young's modulus tends to zero relatively to the shear modulus.

As seen from the graphs, the agreement between analytically and numerically obtained data is very good for higher values of ι_r. On the other hand, the analytical formula underestimates the actual (numerically determined) values of Poisson's ratio and overestimates the actual values of Young's modulus for $\iota_r < 1.3$. For all values of ι_r, the value of Poisson's ratio in the limit case for $\bar{G}/\bar{E} \to \infty$ ($\bar{E} = 0$) is -1 (the extreme theoretical value for Poisson's ratio), while the maximum attainable value is $\frac{1}{4}$ for higher values of ι_r, which corresponds analytically derive formulas. A higher value of Poisson's ratio, up to 0.335, is obtained for $\iota_r = 1.05$.

3.2 DEM–FEM coupling

3.2.1 Surface couupling

This very simple example is aimed to test the approach, mainly correct contact detection and interaction evaluation. A cantilever is "bombarded" by three particles. One particle hits the cantilever "directly", while two particles hit the cantilever outside its original position (one aspect of the testing). The cantilever is modeled by FEM with linear brick elements. The bottom of the cantilever has fixed displacements. The cantilever surface (set of quadrilateral faces) is triangulated and copied to the DEM part of the simulation. The DEM "impactors" can have different shapes, e.g., spherical or polyhedral. The visual results are shown in figure 3.4.

3.2.2 Volume coupling

In this example, a simply supported 2D beam subjected to a missile impact was simulated. The sides of the beam body were simulated by FEM as a plane stress problem using

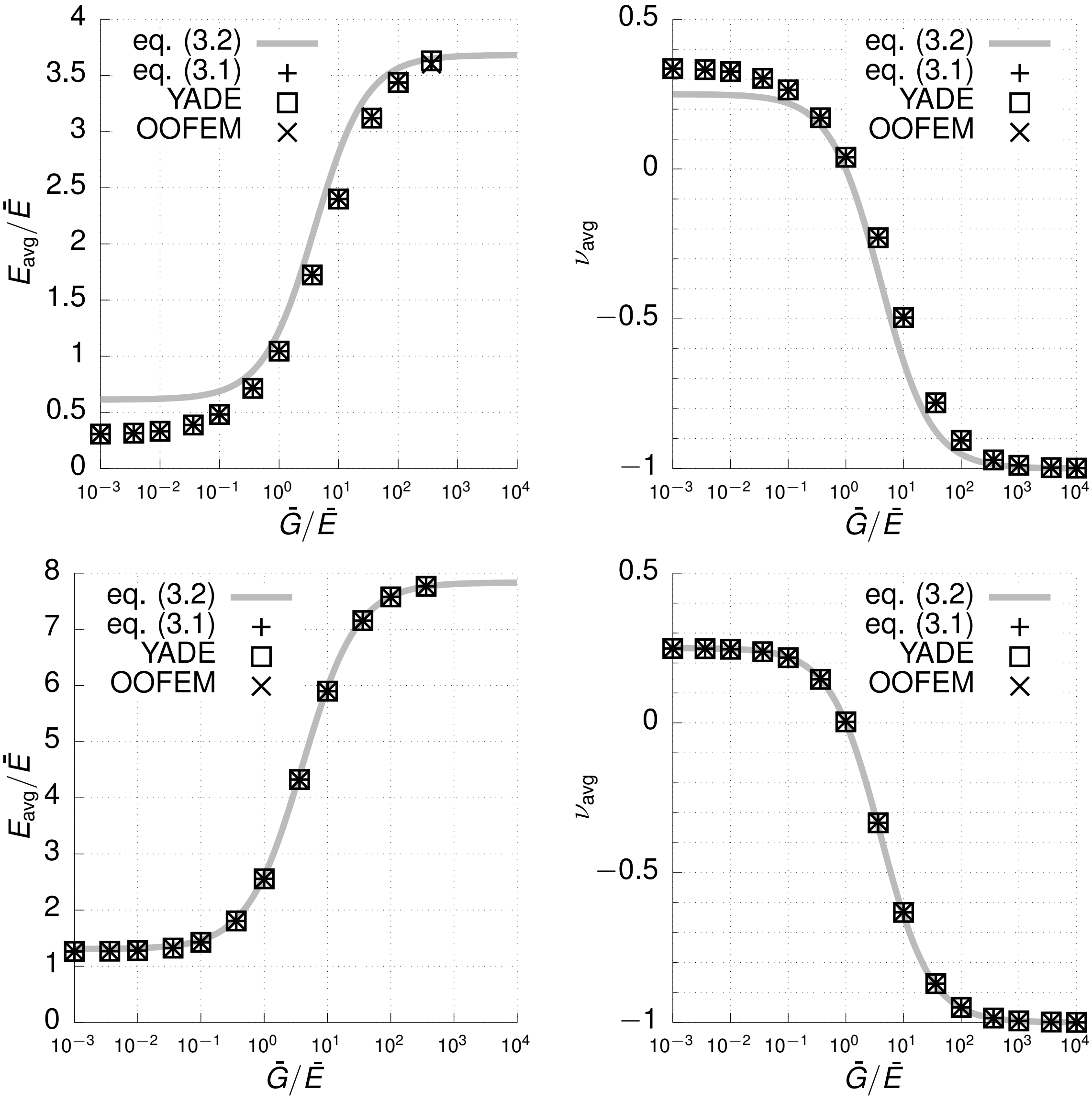

Figure 3.1: Relation between macro- and microscopic parameters for ι_r = 1.05 (top) and ι_r = 1.50 (bottom)

quadrilateral elements linear elastic material law. The central part was modeled by DEM using a regular packing and CPM material model. The material parameters and initial conditions are artificially set to get “nice” results. The visual results are shown in figure 3.2.

3.2.3 Multiscale coupling

Uniaxial strain (oedometric test) of a sample consisting of three different (linear elastic) materials is simulated in this example. The macro-scale problem is modeled by three brick elements. Each FEM element has eight integration points. The upper one is a pure FEM element. For each integration point of the two bottom elements, different DEM micro-scale RVE simulations are performed.

The visual results are shown in figure 3.5. In each “DEM” element, one micro RVE result is displayed. The results of linear elastic behavior are not extremely spectacular indeed, but using a nonlinear behavior of RVEs (resulting in a higher stiffness when more inter-particle contacts occur for instance) could be very useful for certain applications.

3.2.4 Contact coupling

In this example, collision of three elastic bodies is presented. All three particles are modeled by FEM, only a detection algorithm is borrowed from DEM. The visual results are shown in figure 3.3.

3.3 Sequential coupling - uniaxial compression

In this section, the results of proposed sequential coupling method are shown on simple “one element” tests. The simulated prismatic specimen is subjected to uniaxial compression. In the case of a one-element FEM simulation, the definition of boundary conditions is straightforward. In the DEM simulation, the axial strain is imposed by prescribed displacements at the top and bottom boundary layers. In the lateral directions, the particles are free to move. For the graphical post-processing, the stress values from DEM simulation are obtained as the normal component in the axial direction of the average stress.

The DEM and FEM material parameters are set such that the resulting stress-strain diagrams are as similar as possible. Figure 3.6 shows a very good agreement of the two models in both pre-peak and post-peak regime. However, the two models differ at the peak load (the CPM softening starts prior to the DPM softening).

The DEM specimen is loaded at a certain level and then possibly unloaded. At the final stage of the DEM simulation, relevant quantities are mapped onto the one-element FEM simulation and the FEM simulation is run. The average stress tensor and average damage tensor are evaluated from all “ordinary” particles (not belonging to the layer imposing boundary conditions).

Graphs in figures 3.6 show results of the CPM simulation (grey) and continuation with the mapped DPM model (black). The presented results show a reasonable approximation of the FEM behavior after the transformation from DEM. The biggest error is obtained, if the mapping occurs around the peak (or after unloading from around the peak) where the results of two presented models differ the most.

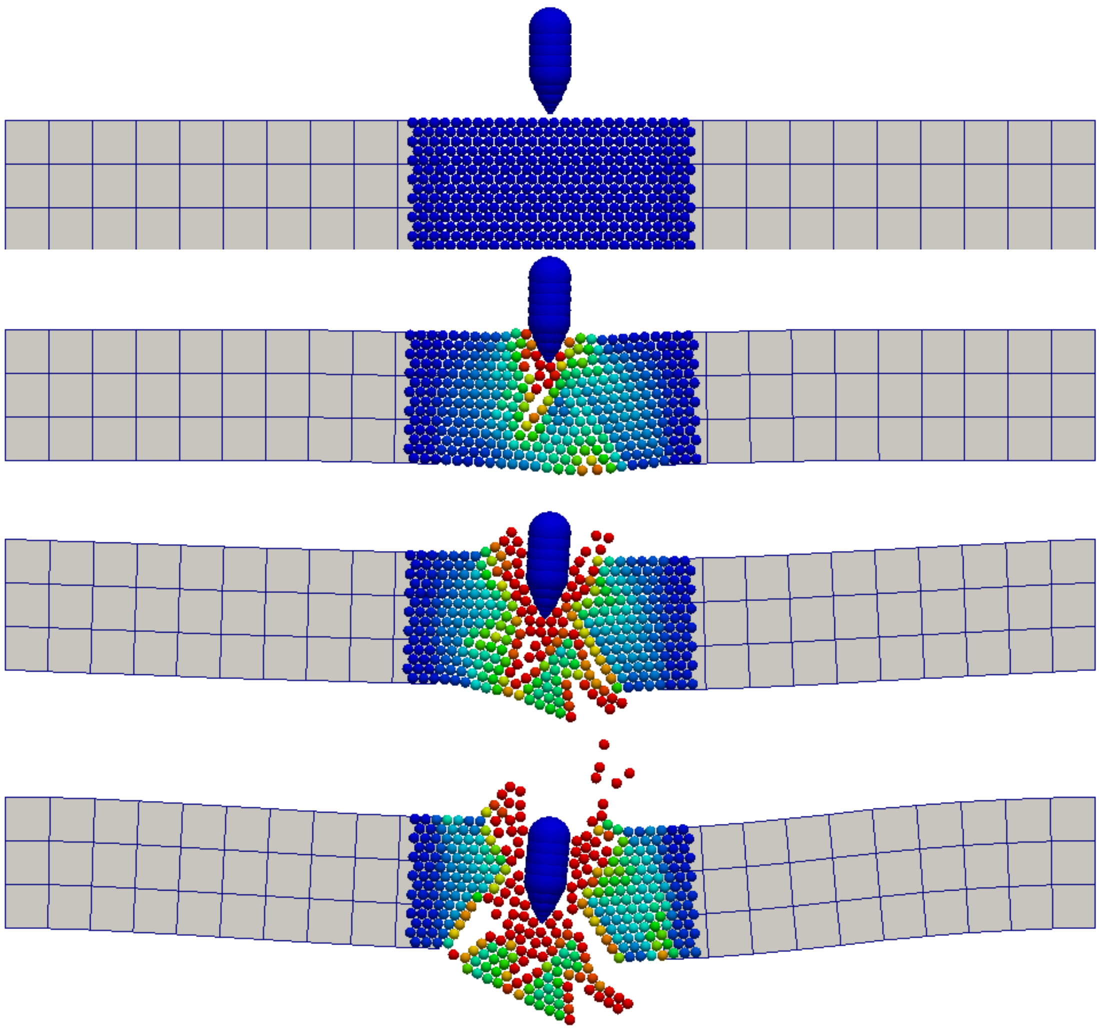

Figure 3.2: Impact on a simply supported beam at different stages

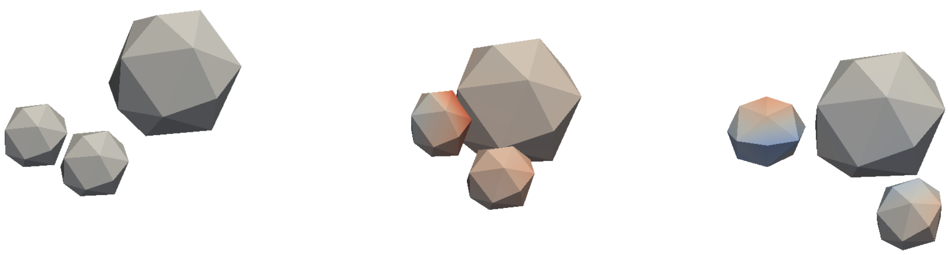

Figure 3.3: Collision of three elastic particles at different stages

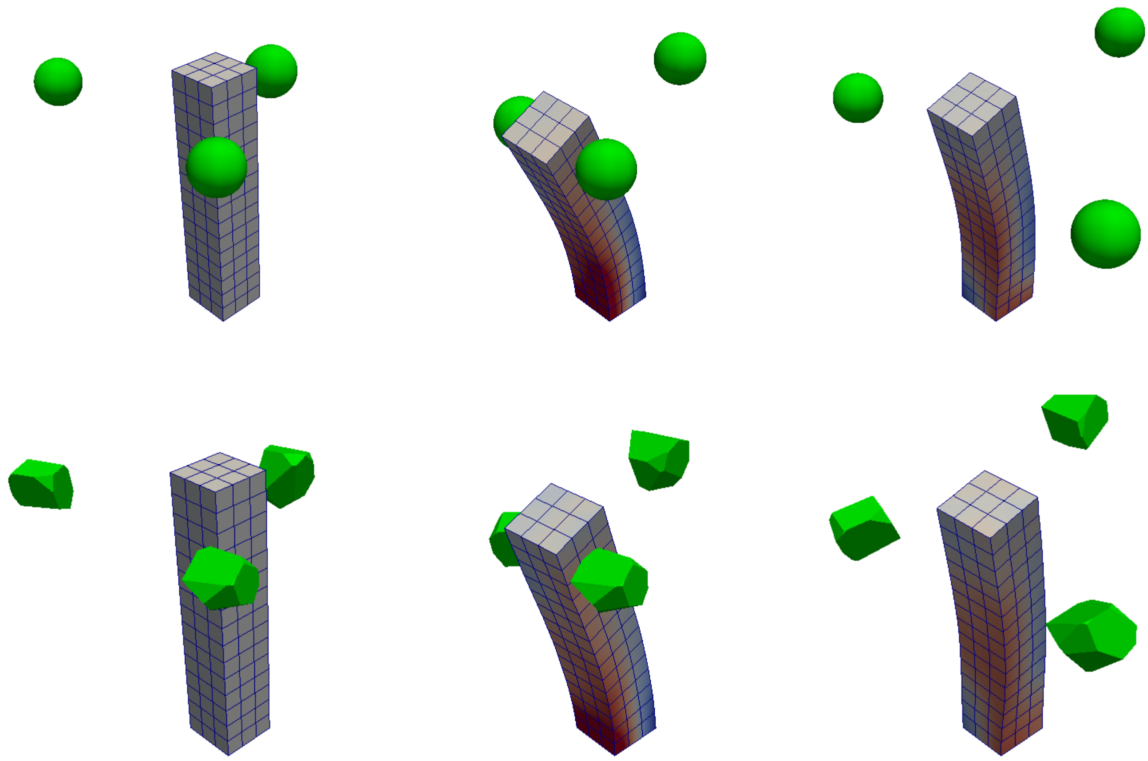

Figure 3.4: Impact on a cantilever at different stages. DEM particles can be spheres (top) or polyhedrons (bottom).

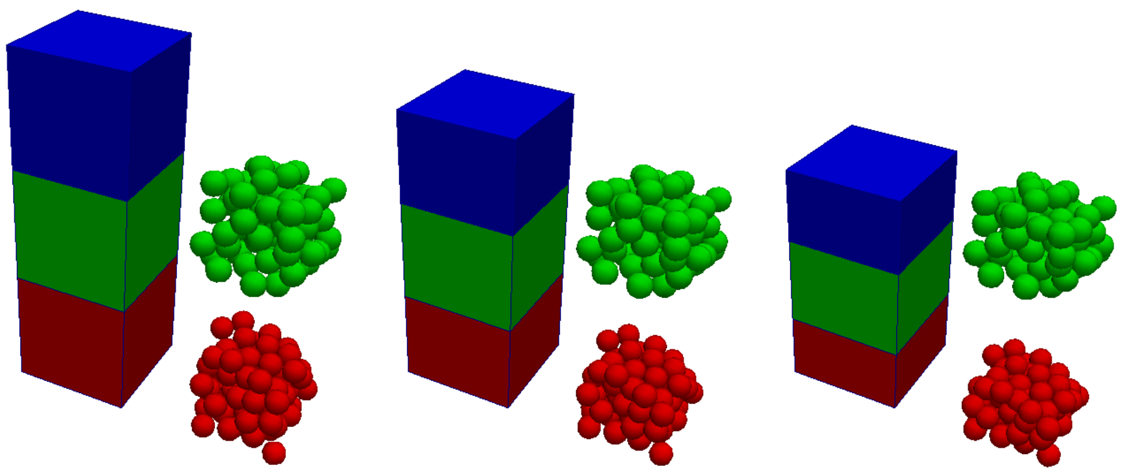

Figure 3.5: Uniaxial strain test at different stages

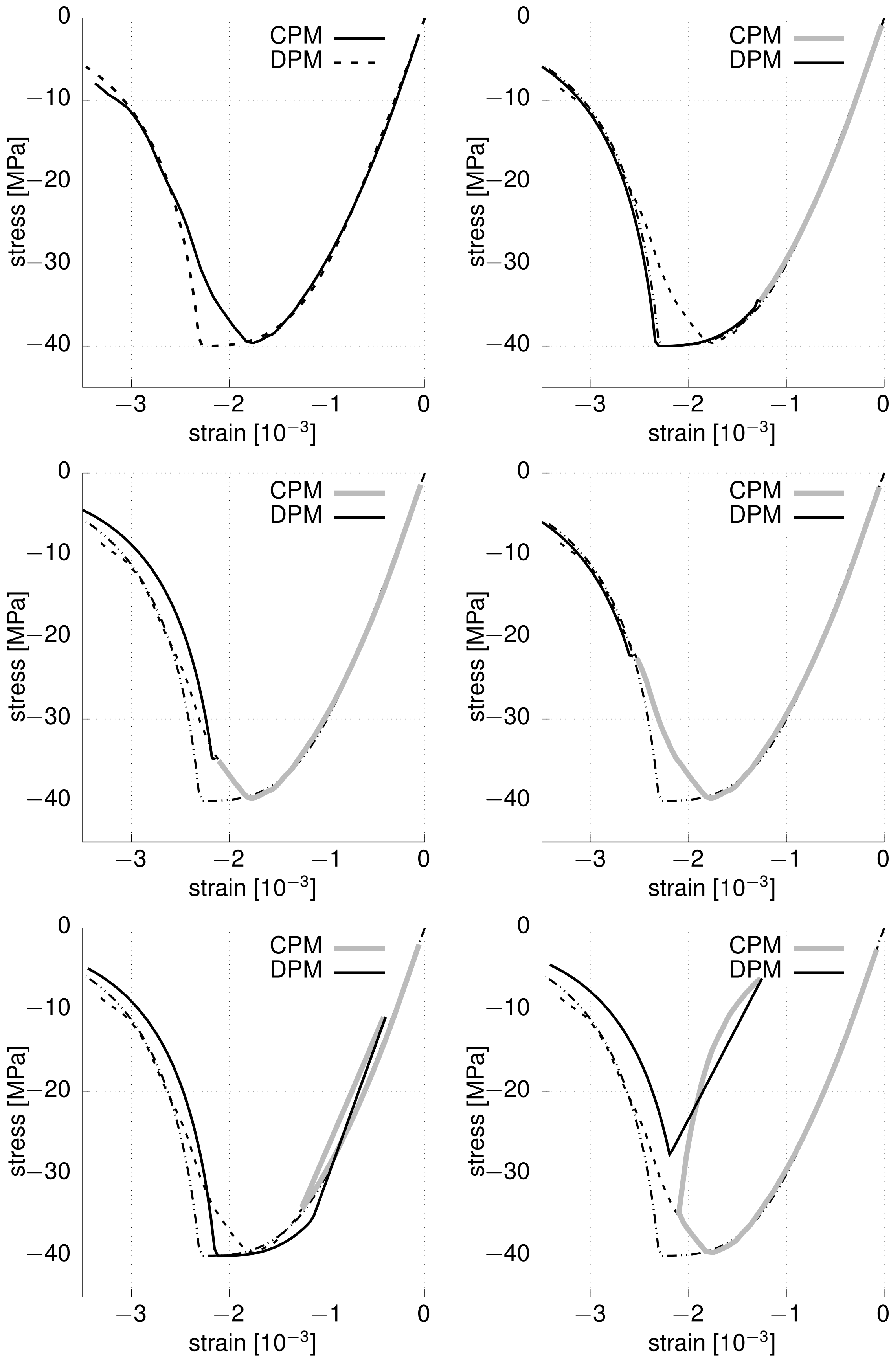

Figure 3.6: Results of sequential coupling

3.4 Discrete mesoscale model for concrete - experiment [8, 9, 33]

From the studied literature, the experiment from [8, 9, 33] was chosen for validation. The experiments investigate the influence of different aggregate sizes (different grading curves) on concrete material properties (f_t, f_c, G_f, E). Two concrete compositions (low strength and high strength) are examined, each with three different aggregate grading curves.

Figures 3.7 show the comparison between simulations and experimental data. Since the absolute values of macroscopic quantities can be relatively easily estimated, only values relative to the results for the smallest aggregate size are plotted.

Each point in the graphs is the averaged simulation result from 3 runs. For each run, the same aggregate sizes were considered (according to the corresponding concrete composition and grading curve) and their positions were chosen randomly. The simulations were performed on 50 mm cubic samples with 2 mm DEM particle size (diameter).

Several combinations of input parameters were tested. The results are plotted for aggregates 2.5 time stiffer and 5 time stronger than matrix and for ITZ 2 times less stif and 2 times weaker than mortar links. Results 2 refer to 2 times more brittle ITZ than results 1.

The model results reasonably correspond to the trends observed in the experiments, although the precise values are fitted with a certain discrepancy.

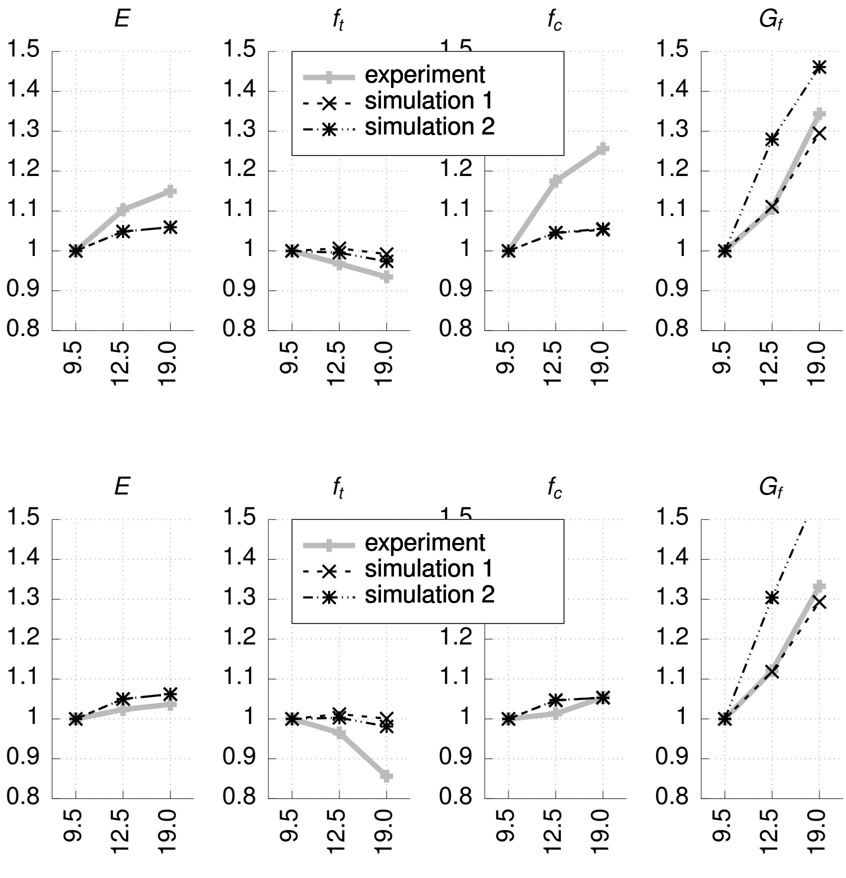

Figure 3.7: Comparison of simulations and experiment [8, 9, 33] for low strength (top) and high strength (bottom) concrete.

4 Conclusions

The following research objectives were accomplished in the present thesis:

- The relation between micro- and macroscopic elastic parameters was investigated both analytically and numerically. The analytical formulas were derived based on the microplane theory. The numerical results were obtained by DEM and FEM simulations. Very good correspondence of the numerical and analytical results is found for packings with interaction ratio greater than 1.25. For lower values of the interaction ratio, the analytical estimation of Young's modulus and Poisson's ratio based on the assumption of uniform distribution of directions of links differs from the numerical results. However, the analytical formula for the full stiffness tensor corresponds to the numerical results very well for all tested values of the interaction ratio.

- The derivation of the stress tensor and couple stress tensor based on the virtual work principle was reviewed and new formulas for the couple stress tensor were proposed and discussed. For the defined volume, the new formulas yield a unique value of the couple stress tensor independent of the choice of the coordinate reference point, which (according to the author's knowledge) has not yet been published in the literature.

- Various classes of FEM–DEM concurrent coupling strategies (namely the surface, direct volume, multiscale and contact coupling) were described. Existing software packages OOFEM and YADE (both providing Python user interface) were chosen for the coupling. Each strategy was illustrated on a simple example. The examples together with the unifying framework form a new open source code project.

- A mapping of the final state of a DEM simulation onto the initial state of the FEM simulation (also referred to as a sequential coupling) was illustrated on uniaxial compression of a concrete material. The method was proven to be able to capture the transition from DEM to FEM relatively well for several different loading scenarios – mapping at different stages (elastic range, peak load, softening regime, with or without unloading etc.). The most divergent results were obtained for the stages of loading where the DEM and FEM material models themselves differed the most.

- A new discrete element model for concrete taking into account the heterogeneous mesoscale structure of concrete (i.e., aggregates and ITZ between aggregates and matrix) was proposed and tested. The validation against experimental data from the literature shows the ability of the model to realistically capture trends of various material properties (elastic modulus, tensile and compressive strength, fracture energy) with respect to the actual mesoscale structure of the material.

5 References

[1] F. Alonso-Marroquin. Static equations of the Cosserat continuum derived from intra-granular stresses. *Granular matter* 13 (2011), pp. 189–196.

[2] N. M. Azevedo and J. V. Lemos. Hybrid discrete element/finite element method for fracture analysis. *Computer Methods in Applied Mechanics and Engineering* 195 (2006), pp. 4579–4593.

[3] K. Bagi. Discussion on "The asymmetry of stress in granular media". *International Journal of Solids and Structures* 40 (2003), pp. 1329–1331.

[4] K. Bagi. Stress and strain in granular assemblies. *Mechanics of Materials* 22 (1996), pp. 165–177.

[5] J.-P. Bardet and I. Vardoulakis. Reply to discussion by Dr. Katalin Bagi. *International Journal of Solids and Structures* 40 (2003), p. 1035.

[6] J.-P. Bardet and I. Vardoulakis. Reply to Dr. Kuhn's discussion. *International Journal of Solids and Structures* 40 (2003), p. 1809.

[7] J.-P. Bardet and I. Vardoulakis. The asymmetry of stress in granular media. *International Journal of Solids and Structures* 38.2 (2001), pp. 353–367.

[8] M. H. A. Beygi, M. T. Kazemi, J. V. Amiri, I. M. Nikbin, S. Rabbanifar, and E. Rahmani. Evaluation of the effect of maximum aggregate size on fracture behavior of self compacting concrete. *Construction and Building Materials* 55 (2014), pp. 202–211.

[9] M. H. A. Beygi, M. T. Kazemi, I. M. Nikbin, J. V. Amiri, S. Rabbanifar, and E. Rahmani. The influence of coarse aggregate size and volume on the fracture behavior and brittleness of self-compacting concrete. *Cement and Concrete Research* 66 (2014), pp. 75–90.

[10] O. Buyukozturk and B. Hearing. Crack Propagation in Concrete Composites Influenced by Interface Fracture Parameters. *International Journal of Solids and Structures* 35.31–23 (1998), pp. 4055–4066.

[11] A. Caballero, K. Willam, and I. Carol. Consistent tangent formulation for 3D interface modeling of cracking/fracture in quasi-brittle materials. *Computer Methods in Applied Mechanics and Engineering* 197 (2008), pp. 2804–2822.

[12] F. Camborde, C. Mariotti, and F. Donzé. Numerical study of rock and concrete behaviour by discrete element modelling. *Computers and Geotechnics* 27 (2000), pp. 225–247.

[13] C. S. Chang and M. R. Kuhn. On virtual work and stress in granular media. *International Journal of Solids and Structures* 42 (2005), pp. 3773–3793.

[14] G. Cusatis. "Tridimensional random particle model for concrete". PhD thesis. Polytechnic University of Milan, 2001.

[15] J. B. D. Asahina a E.N. Landis b. Modeling of phase interfaces during pre-critical crack growth in concrete. *Cement & Concrete Composites* 33 (2011), pp. 966–977.

[16] 3. E N Landis1 and J. E. Bolander. Explicit representation of physical processes in concrete fracture. *Journal of Physics D: Applied Physics* 42.21 (2009).

[17] S. Erdem, A. R. Dawson, and N. H. Thom. Influence of the micro- and nanoscale local mechanical properties of the interfacial transition zone on impact behavior of concrete made with different aggregates. *Cement and Concrete Research* 42 (2012), pp. 447–458.

[18] A. Fakhimi. A hybrid discrete–finite element model for numerical simulation of geomaterials. *Computers and Geotechnics* 36 (2009), pp. 386–395.

[19] G. Frenning. An efficient finite/discrete element procedure for simulating compression of 3D particle assemblies. *Computer Methods in Applied Mechanics and Engineering* 197 (2008), pp. 4266–4272.

[20] E. Garboczi. Three-dimensional mathematical analysis of particle shape using X-ray tomography and spherical harmonics: Application to aggregates used in concrete. *Cement and Concrete Research* 32 (2002), pp. 1621–1638.

[21] M. G. D. Geers, V. G. Kouznetsova, and W. A. M. Brekelmans. Multi-scale computational homogenization: Trends and challenges. *Journal of Computational and Applied Mathematics* 234 (2010), pp. 2175–2182.

[22] G. Giaccio, R. Zerbino, J. M. Ponce, and O. R. Batic. Mechanical behavior of concretes damaged by alkali-silica reaction. *Cement and Concrete Research* 38 (2008), pp. 993–1004.

[23] P. Grassl and M. Jirásek. Meso-scale approach to modelling the fracture process zone of concrete subjected to uniaxial tension. *International Journal of Solids and Structures* 47 (2010), pp. 957–968.

[24] U. Groh, H. Konietzky, K. Walter, and M. Herbst. Damage simulation of brittle heterogeneous materials at the grain size level. *Theoretical and Applied Fracture Mechanics* 55 (2011), pp. 31–38.

[25] S. Häfner, S. Eckardt, T. Luther, and C. Könke. Mesoscale modeling of concrete: Geometry and numerics. *Computers and Structures* 84 (2006), pp. 450–461.

[26] S. Hentz, F. V. Donzé, and L. Daudeville. Discrete element modelling of concrete submitted to dynamic loading at high strain rates. *Computers and Structures* 82 (2004), pp. 2509–2524.

[27] A. Ibrahimbegovic and A. Delaplace. Microscale and mesoscale discrete models for dynamic fracture of structures built of brittle material. *Computers and Structures* 81 (2003), pp. 1255–1265.

[28] S.-M. Kim and R. K. A. Al-Rub. Meso-scale computational modeling of the plastic-damage response of cementitious composites. *Cement and Concrete Research* 41 (2011), pp. 339–358.

[29] M. R. Kuhn. Discussion on “The asymmetry of stress in granular media”. *International Journal of Solids and Structures* 40 (2003), pp. 1805–1807.

[30] A. Kwan, Z. Wang, and H. Chan. Mesoscopic study of concrete II: nonlinear Finite element analysis. *Computers and Structures* 70 (1999), pp. 545–556.

[31] A. E. H. Love. *A Treatise on the Mathematical Theory of Elasticity (4th ed.)* Cambridge, University press, 1927.

[32] H. Nakashima and A. Oida. Algorithm and implementation of soil–tire contact analysis code based on dynamic FE–DE method. *Journal of Terramechanics* 41 (2004), pp. 127–137.

[33] I. M. Nikbin, M. H. A. Beygi, M. T. Kazemi, J. V. Amiri, E. Rahmani, S. Rabbanifar, and M. Eslami. A comprehensive investigation into the effect of aging and coarse aggregate size and volume on mechanical properties of self-compacting concrete. *Materials and Design* 59 (2014), pp. 199–210.

[34] E. Onate and J. Rojek. Combination of discrete element and finite element methods for dynamic analysis of geomechanics problems. *Computer Methods in Applied Mechanics and Engineering* 139 (2004), pp. 3087–3128.

[35] R. Pedersen, A. Simone, and L. Sluys. Mesoscopic modeling and simulation of the dynamic tensile behavior of concrete. *Cement and Concrete Research* 50 (2013), pp. 74–87.

[36] J. Rojek and E. Onate. Multiscale analysis using a coupled discrete/finite element model. *Interaction and Multiscale Mechanics* 1 (2007), pp. 1–31.

[37] J. Rousseau, E. Frangin, P. Marin, and L. Daudville. Multidomain finite and discrete elements method for impact analysis of a concrete structure. *Engineering Structures* 31 (2009), pp. 2735–2743.

[38] D. Rypl. Using the spherical harmonic analysis and the advancing front technique for the discretization of 3D aggregate particles. *Advances in Engineering Software* 41 (2010), pp. 38–45.

[39] A. Satoh, K. Yamada, and S. Ishiyama. Simplified two-dimensional mesoscopic model for evaluating mechanical properties and crack paths near interfaces in concrete. *Engineering Fracture Mechanics* 4 (2013), pp. 6–20.

[40] J. Stránský and M. Jirásek. “Calibration of particle-based models using cells with periodic boundary conditions”. In: *Particle-based Methods II - Fundamentals and Applications*. Ed. by E. Oñate and D. R. J. Owen. Barcelona, Spain: CIMNE, 2011, pp. 274–285.

[41] V. T. Tran, F. V. Donzé, and P. Marin. A discrete element model of concrete under high triaxial loading. *Cement & Concrete Composites* 33 (2011), pp. 936–948.

[42] N. Tregger, D. Corr, L. Graham-Brady, and S. Shah. Modeling the effect of mesoscale randomness on concrete fracture. *Probabilistic Engineering Mechanics* 21 (2006), pp. 217–225.

[43] Z. Wang, F. Lin, and X. Gu. Numerical Simulation of Failure Process of Concrete Under Compression Based on Mesoscopic Discrete Element Model. *Tsinghua Science And Technology* 13.S1 (2008), pp. 19–25.

[44] C. Wellmann and P. Wriggers. Atwo-scalemodel of granularmaterials. *Computer Methods in Applied Mechanics and Engineering* 205–208 (2012), pp. 46–58.

[45] P. Wriggers and S. Moftah. Mesoscale models for concrete: Homogenisation and damage behaviour. *Finite Elements in Analysis and Design* 42 (2006), pp. 623–636.

[46] M. Xu, R. Gracie, and T. Belytschko. “Bridging the Scales in Science and Engineering”. In: ed. by J. Fish. Oxford University Press, 2002. Chap. Multiscalemodelingwith extended bridging domain method.

[47] X. Zhou and H. Hao. Mesoscale modelling of concrete tensile failure mechanism at high strain rates. *Computers and Structures* 86 (2008), pp. 2013–2026.

6 Selected publications of the author

Journal papers

[1] W. Song, B. Huang, X. Shu, J. Stránský, and H. Wu. Interaction between railroad ballast and sleeper: a DEM-FEM approach. *International Journal of Geomechanics* (submitted).

Conference papers

[1] J. Stránský, M. Jirásek, and V. Šmilauer. “Macroscopic Elastic Properties of Particle Models”. In: *Modelling and Simulation 2010*. Prague, Czech Republic, 2010.

[2] J. Stránský, M. Jirásek, and V. Šmilauer. “Macroscopic Properties of Particle Models: Uniaxial Tension”. In: *Nano and Macro Mechanics 2010*. Prague, Czech Republic, 2010.

[3] J. Stránský and M. Jirásek. “Calibration of Particle Models using Cells with Periodic Boundary Conditions”. In: *Particles 2011*. Barcelona, Spain, 2011.

[4] J. Stránský and M. Jirásek. “Inelastic Calibration of Particle Models using Cells with Periodic Boundary Conditions”. In: *Nano and Macro Mechanics 2011*. Prague, Czech Republic, 2011.

[5] J. Stránský and M. Jirásek. “Open Source FEM-DEM Coupling”. In: *Engineering Mechanics 2012*. Svratka, Czech Republic, 2012.

[6] J. Stránský and M. Jirásek. “Review on evaluation fo equivalent stress tensor in the discrete element method”. In: *Nano and Macro Mechanics 2012*. Prague, Czech Republic, 2012.

[7] J. Stránský. “Open Source DEM-FEM Coupling”. In: *Particles 2013*. Stuttgart, Germany, 2013.

[8] J. Stránský. “Combination of FEM and DEM with Application to Railway Ballast-Sleeper Interaction”. In: *Engineering Mechanics 2014*. Svratka, Czech Republic, 2014.

[9] J. Stránský. “Stochastic Wang tiles generation using DEM and YADE software”. In: *Nano and Macro Mechanics 2014*. Prague, Czech Republic, 2014.

[10] J. Stránský and M. Doškář. “Comparison of DEM-based Wang tilings and PUC”. In: *Nano and Macro Mechanics 2015*. Prague, Czech Republic, 2015.

[11] J. Stránský and M. Doškář. “Stochastic Wang tiles generation using the discrete element method”. In: *Engineering Mechanics 2015*. Svratka, Czech Republic, 2015.

Other

[1] V. Šmilauer, E. Catalano, B. Chareyre, S. Dorofeenko, J. Duriez, N. Dyck, J. Eliáš, B. Er, A. Eulitz, A. Gladky, C. Jakob, F. Kneib, J. Kozicki, D. Marzougui, R. Maurin, C. Modenese, L. Scholtès, L. Sibille, J. Stránský, T. Sweijen, K. Thoeni, and C. Yuan. “Reference Manual”. In: *Yade Documentation 2nd ed.* http://yade-dem.org/doc/. The Yade Project, 2015. DOI: `10.5281/zenodo.34045`.

7 Abstract

The presented thesis deals with various aspects of the discrete element method (DEM) with application to modeling of concrete failure and combination of DEM with the finite element method (FEM).

Basic properties (e.g., isotropy) of random densely packed particle assemblies (as a usual initial DEM packing configuration) are analyzed for various numbers of particles. Elastic properties of such packings are investigated both analytically and numerically. The analytical formulas are derived based on the microplane theory. The numerical results are obtained by DEM and FEM simulations. A very good agreement between analytical and numerical results is found for interaction ratios greater than 1.25. For lower values of the interaction ratio, the analytically derived full stiffness tensor corresponds to the numerical results very well, however, the values of Young's modulus and Poisson's ratio estimated based on the assumption of uniform distribution of link directions exhibit a certain discrepancy from the numerical results.

The discrete nature is an essential feature of DEM. However, in some cases it is desirable to transform such discrete information (contact forces for instance) into its continuum counterpart (e.g., stress tensor). The evaluation of the stress tensor and couple stress tensor from discrete forces based on the principle of virtual work is reviewed. New formulas for the couple stress tensor, yielding a unique value of the couple stress tensor independent on the choice of the coordinate reference point, are presented and discussed.

Both DEM and FEM have their fields of application, however, in certain cases they can be combined and used together. In the concurrent coupling approach, both DEM and FEM simulations are run at the same time. Coupling of FEM code OOFEM and DEM code YADE is described. Several classes of coupling approaches (namely surface, direct volume, multiscale and contact) are addressed and illustrated on simple examples.

A DEM to FEM sequential coupling (in which case the DEM simulation is run first and the resulting state is converted into an initial state of the FEM simulation) of damaged concrete material is presented for the case of uniaxial compression. The method is proven to be able to capture the transition from DEM to FEM relatively well for several different loading scenarios – mapping at different stages (elastic range, peak load, softening regime, with or without unloading etc.). The most divergent results are obtained for the stages of loading where the DEM and FEM material models themselves differ the most.

In practical civil engineering, concrete is usually idealized as a homogeneous isotropic material. However, certain applications require description of concrete on a lower scale and heterogeneity has to be taken into account. The development and results of a new mesoscale discrete element model for concrete is described. The model takes into account the heterogeneous mesoscale structure of concrete (i.e., aggregates and interfacial transition zone between aggregates and matrix). The validation against experimental data from literature shows the ability of the model to realistically capture trends of various material properties (elastic modulus, tensile and compressive strength, fracture energy) with respect to the actual mesoscale structure of the material. *Keywords:* Discrete Element

Method, Finite Element Method, multimethod coupling, Python, concrete, mesoscale